$CaAl_2Si_2O_8$: Ce^{3+}, Tb^{3+}: A novel high-efficiency luminescent material for white light-emitting diodes

Haiyan Jiao[1, *], Qiong Chen[1, a] and Peiyu Wang[1, b]

College of Electric Engineering, Northwest MinZu University, Lanzhou, China

*Corresponding author e-mail: dqjhy@xbmu.edu.cn, [a]115416333@qq.com, [b]479478559 @qq.com

Abstract. A novel rare earth activated phosphor $Ca_{1-x-y}Al_2Si_2O_8$:xCe^{3+}, yTb^{3+} were prepared under a weak reducing atmosphere by conventional solid-state reaction method and their luminescence properties under 351 nm excitation were investigated in detail. The results show that the $CaAl_2Si_2O_8$: Tb^{3+} shows excited at short-UV region, the long-UV absorption peaks is very weak, which cannot be effectively excited by near ultraviolet light-emitting diodes (NUV-LEDs). However, by incorporation of Ce^{3+}, in the excitation spectra, strong and broad excitation bands at ~ 351nm were observed, which could well match with the emission wavelength of the NUV-LEDs chip. Simultaneity, the green characteristic emission of Tb^{3+} is obviously enhanced, and the emission intensity of $CaAl_2Si_2O_8$:Ce^{3+}, Tb^{3+} phosphor is 10 times higher than that of the green phosphor $CaAl_2Si_2O_8$:Tb^{3+} phosphor. The results indicates an efficient energy transfer from Ce^{3+} to Tb^{3+} was found and the energy transfer mechanism of $Ce^{3+} \rightarrow Tb^{3+}$ was studied in detail.

1. Introduction

In the global energy crisis, environments under the condition of constantly improve, the miniaturization of semiconductor light-emitting diodes (LEDs) lighting have been recognized as a new generation of lighting source due to their superior features of long life, energy saving, safety and environmental friendliness , which have attracted more and more attention of people [1, 2]. At present, the main strategy to obtain the commercialization of white light-emitting diodes (LEDs) is the combination of blue LED chip with $Y_3Al_5O_{12}$:Ce^{3+} (YAG: Ce) yellow phosphor. Although this device have high luminous efficiency (the latest record has topped 300 lm/W), which is far higher than that of the traditional incandescent lamp (about 16 lm/W) and fluorescent lamp (about 70 lm/W), but this method suffers the problems of high correlated color temperature (T_c >5000 K) and low color rendering index (R_a < 70) for general illumination due to the insufficient red-light contribution [3]. In order to solve this problem and produce white light with suitable correlated color temperature (CCT) and excellent color rendering index (CRI), trichromatic white LEDs have been proposed by pumping the tricolor (red, green and blue) phosphors with near-ultraviolet (NUV) LED chips [4]. Thus, the white light LEDs luminous efficiency and CRI strongly depends on the tricolor phosphors, the luminescence properties of phosphor plays a key role for "phosphor-converted" technology in the white light LEDs. At present, the commercial green phosphor is ZnS: Cu^+, Al^{3+}, but the sulfide phosphors has a bad stability in air, easily deliquescence, and which is easy to decompose and produce harmful gases. So the application of sulfide phosphors are

limited [5]. In recent years, nitride and nitrogen oxides have been widely studied because of their excellent luminescent properties, but the development of these phosphors is greatly restricted by the harsh preparation conditions [6]. In this regard, it is essential to develop a novel green phosphors which can be efficiently excited by the NUV- LED chips.

Over the past few decades, about the $Ce^{3+}\rightarrow Tb^{3+}$energy transfer of luminescence materials have been widely research [7-9], which is mainly focused on the study of new and efficient green phosphors as the green components of low-pressure mercury vapor fluorescent lamps. Because Tb^{3+} ion is a good activator with green characteristic emission, its f-f absorption in the long wave ultraviolet region is usually relatively weak and cannot be effectively excited by near ultraviolet LED chips. Considering that Ce^{3+} is not only an efficient luminescent center, but also a good sensitizer, which can effectively sensitize the luminescence center of Tb^{3+}. In theory, there is energy transfer in $Ce^{3+}\rightarrow Tb^{3+}$, but the energy transfer efficiency is different in different host systems. Alkaline-earth aluminum silicate is an important mineral resource. It has been widely used in petroleum, plastics processing, building materials and light industry. In recent years, its research as the substrate of luminescent materials has attracted much attention. Alkaline-earth aluminum silicate belongs to feldspar, in which anorthite $CaAl_2Si_2O_8$ belongs to triclinic system. Essentially, the structures of alkaline-earth metal aluminum silicates are based on an infinite three-dimensional silicon–oxygen and aluminum–oxygen frameworks, which are formed from interlinked corner-sharing $[SiO_4]^{4-}$ and $[AlO_4]^{5-}$ tetrahedral [10,11]. This structure has large crystal cells and a variety of positions for different ions. Most of the research on this system is focused on the application of crystal and glass ceramics, but less on the substrate of luminescent materials. It is reported that there is a study on the luminescence properties of blue phosphor $(Ca_{1-x}Mg_x)$ $Al_2Si_2O_8$: Eu^{2+} in PDP [12], and the blue long afterglow material of $CaAl_2Si_2O_8$:Eu^{2+}, Dy^{3+} [13, 14]. However, the energy transfer process and luminescence kinetics of $Ce^{3+}\rightarrow Tb^{3+}$have not been reported.

Therefore, in this paper, $CaAl_2Si_2O_8$:Ce^{3+}, Tb^{3+} phosphors were synthesized by high temperature solid phase method and the luminescence properties in NUV region were investigated. We focused on the concentration change and energy transfer of $Ce^{3+}\rightarrow Tb^{3+}$, trying to increase the absorption peak of near ultraviolet (330 ~ 410nm) through Ce^{3+} to Tb^{3+} energy transfer. A new and efficient green phosphor for near ultraviolet LED has been developed.

2. Experimental

2.1. Materials and synthesis

A series powder samples $Ca_{0.95-x}Al_2Si_2O_8$:xCe^{3+} (CAS: xCe^{3+}) ($0.005\leq x\leq 0.06$) and $Ca_{0.95-x}Al_2Si_2O_8$:xCe^{3+}, $0.05Tb^{3+}$ (CAS: xCe^{3+}, $0.05Tb^{3+}$) ($0\leq x\leq 0.06$) were prepared by a traditional high temperature solid-state reaction process. Stoichiometric amounts of the starting materials $CaCO_3$ (99 %), Al_2O_3 (99 %), H_2SiO_3, CeO_2 (99.5 %), H_3BO_3 (99.5 %) and Tb_4O_7 (99.99 %) were weighed and blended in agate mortar thoroughly ground for 30min-1 h in alcohol. Subsequently, the dried powder mixture was placed in a alumina crucible and then preheated at 900 ºC for 3 h in air, then fully ground and heated at 1300ºC for 12 h in a weak reductive atmosphere of 5% H_2 - 95% N_2 gas. Finally, the prepared phosphors were cooled to room temperature and reground to get the final phosphors.

2.2. Measurements and characterization

The phase purity of all the synthesized samples were identified by a Rigaku D/Max-2400 powder X-ray diffractometer (XRD) operating at 40 kV/60 mA with Ni-filtered Cu Kα radiation (λ = 1.54056Å). The scanning rate was seted at 10°/ min with 2θ ranges from 10° to 80° with a step size of 0.02°. The Excitation (PLE) and emission (PL) spectra of the samples were measured using an FLS-920T fluorescence spectrophotometer equipped with a 450 W xenon arc lamp light source and double excitation monochromators (Edinburgh Instrument, Britain). All the measurements were performed at room temperature.

3. Results and Disdussion

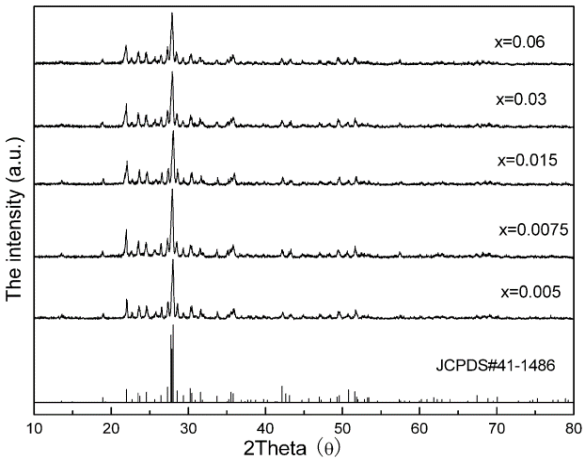

Figure 1. The XRD patterns of $Ca_{1-x}Al_2Si_2O_8$: xCe^{3+} for different Ce^{3+} dopants concentration

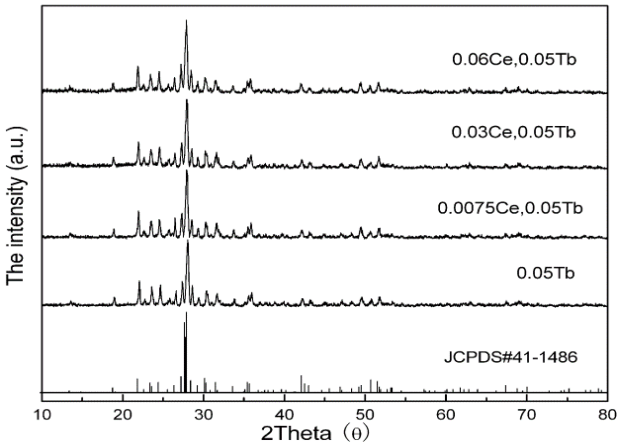

Figure 2. XRD patterns of prepared samples and standard data of $Ca_{0.95-x}Al_2Si_2O_8$: xCe^{3+}, $0.05Tb^{3+}$ ($0 \le x \le 0.06$)

The XRD patterns of $Ca_{1-x}Al_2Si_2O_8$:xCe^{3+} ($0.005 \le x \le 0.06$) for different Ce^{3+} dopants concentration are shown in Fig.1, along with the standard pattern of JCPDS#41-1486 as a reference. The results showed that when the doping concentration of Ce^{3+} was less than 0.06, no other phase was observed, the XRD patterns of obtained samples were in good match with the $CaAl_2Si_2O_8$ phase (JCPDS No.41-1486), which has a triclinic crystal system. Fig.2 shows the powder XRD patterns of doubly doped series sample $Ca_{0.95-x}Al_2Si_2O_8$:xCe^{3+}, $0.05Tb^{3+}$ ($0 \le x \le 0.06$). It can be seen that the X-ray diffraction peak of all samples are consistent with the JCPDS standard card (No.41-1486), confirming the formation of the single-phase nature.

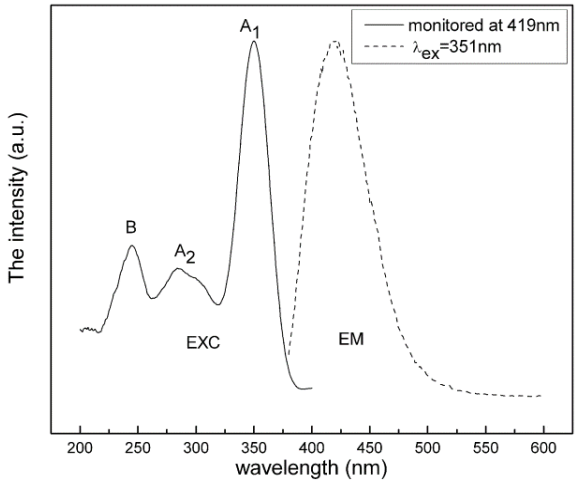

Figure 3. The excitation (λ_{em} = 419 nm) and emission spectra (λ_{ex}=351 nm) for $CaAl_2Si_2O_8$:$0.0075Ce^{3+}$ powders.

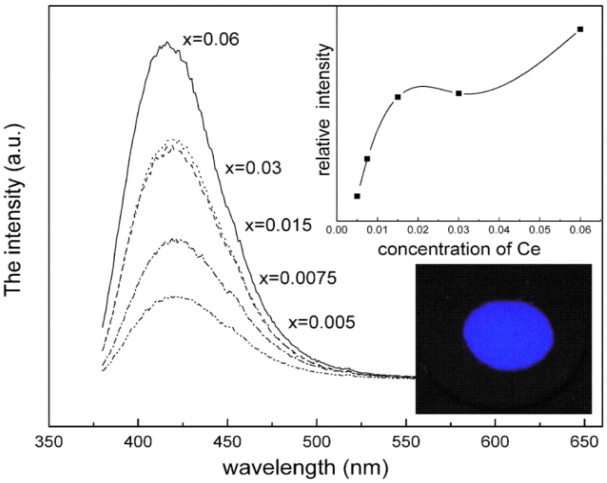

Figure 4. The Emission spectra of $Ca_{1-x}Al_2Si_2O_8$:xCe^{3+}. ($0.005 \le x \le 0.06$) (λ_{ex}=351 nm)

Fig.3 displays the excitation and emission spectra of $CaAl_2Si_2O_8$:$0.0075Ce^{3+}$. The excitation spectrum is composed of three excitation peaks under the monitoring of 419 nm. The main peaks is located at 245 nm, 284 nm and 351 nm, respectively. Among them, the strongest excitation peak is at

351 nm, which belongs to the transition from the ground state of Ce^{3+} to the different splitting energy levels in the 5d excited state, and the splitting of crystal field is ~ 12 400 cm^{-1}. The emission spectrum was excited by 351 nm, shows a broad emission band with a main peak located in the blue violet region at ~ 419 nm (23 866 cm^{-1}), belonging to the 5d→4f ($^2F_{5/2}$ and $^2F_{7/2}$) transition of Ce^{3+}. In addition, when the sample was excited at 245 nm, 284 nm or 351 nm, the shape and peak position of emission spectrum did not change, but the intensity was different. In general, the typical doublet emission bands due to the transition of the Ce^{3+} ions from the 5d excited state to the $^2F_{5/2}$ and $^2F_{7/2}$ ground states, and the energy level difference is about 2000 cm^{-1}. However, there is only one emission band in the system, which indicates that the spin orbit coupling of Ce^{3+} ground state is very weak. Besides, the emission spectrum is slightly asymmetrical towards long wave direction, indicating that the crystal field around Ce^{3+} is stronger than its spin orbit coupling.

Fig.4 shows the emission spectra of $Ca_{1-x}Al_2Si_2O_8:xCe^{3+}$ ($0.005 \le x \le 0.06$) with different concentrations of Ce^{3+} (λ_{ex}=351 nm). It is obviously observed that $Ca_{1-x}Al_2Si_2O_8$: xCe^{3+} can be efficiently excited by UV light and emit the blue light from *5d-4f* transition of Ce^{3+}. With the change of Ce^{3+} doping concentration, the peak shape and position of emission spectra of all samples are consistent. The illustrations show the relationship between the luminescence intensity of a series of samples $Ca_{1-x}Al_2Si_2O_8$: xCe^{3+} ($0.005 \le x \le 0.06$) and the doping concentration of Ce^{3+}. It can be seen that with the increase of Ce^{3+}doping concentration, the luminescence intensity is gradually enhanced, and there is no concentration quenching phenomenon. This phenomenon can be explained that the Stokes shift of Ce^{3+} is relatively large (~ 4624 cm^{-1}) in this system, meaning that the overlap of excitation and emission spectra is very small (~ 0.2 eV^{-1}), which indicates that the non-radiative energy transfer efficiency between adjacent luminescent center ion Ce^{3+} and Ce^{3+} is relatively low. The small illustrations in Fig. 4 give a photo of the sample $CaAl_2Si_2O_8:0.06Ce^{3+}$ with the highest luminescence intensity under the ultraviolet light, which can be seen to emit bright blue light.

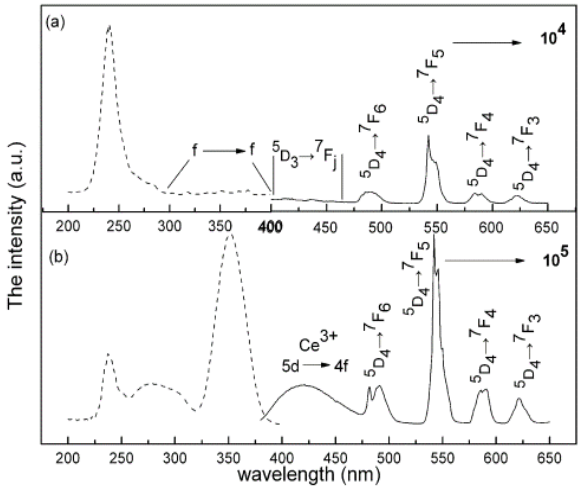

Figure 5. The excitation (λ_{em} = 542 nm) and emission spectra (λ_{ex} = 351 nm) for (a) $CaAl_2Si_2O_8:0.05Tb^{3+}$ and (b) $CaAl_2Si_2O_8:0.06Ce^{3+}$, $0.05Tb^{3+}$.

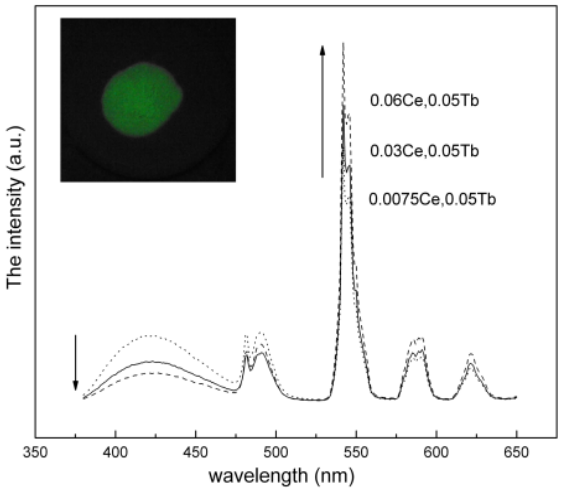

Figure 6. The Emission spectra of $Ca_{0.95-x}Al_2Si_2O_8$: xCe^{3+}, $0.05Tb^{3+}$ ($0.005 \le x \le 0.06$) (λex = 351 nm). The inserted figure shows the photo of. $CaAl_2Si_2O_8$: $0.06Ce^{3+}$, $0.05Tb^{3+}$ under UV

Fig.5 depicts the excitation (λ_{em} = 542 nm) and emission spectra (λ_{ex} = 351 nm) for (a) $CaAl_2Si_2O_8$:0.05 Tb^{3+} and (b) $CaAl_2Si_2O_8:0.06Ce^{3+}$, $0.05Tb^{3+}$. It can be seen from the spectra of single-doped Tb^{3+} (a) that the excitation spectrum consists of two parts: the strong absorption band located in the 200 ~ 280nm short-wave ultraviolet region and the f-f absorption line of the Tb^{3+} ion which is very weak in the 280 ~ 400nm long-wave ultraviolet region. Its emission spectrum includes four emission peaks, the main peaks are 485 nm, 542 nm, 590 nm, 621 nm, corresponding to the $^5D_4 \rightarrow {}^7F_J$ (J= 6, 5, 4,

3) of Tb^{3+}, respectively, in which the $^5D_4$-$^7F_5$ transition intensity of 542nm is the largest, which is the characteristic green emission of Tb^{3+}. If observed carefully, there is a very weak emission peak at 400 ~ 480 nm, which is attributed to the transition $^5D_3 \rightarrow {}^7F_J$ (J= 6, 5, 4, 3, 2, 1) of Tb^{3+}. This has also been reported in other Tb^{3+} doped matrix [15-17], that is, when the doping concentration of Tb^{3+} is low, the transition emission of $^5D_3 \rightarrow {}^7F_J$ and $^5D_4 \rightarrow {}^7F_J$ exists simultaneously. When the doping concentration of Tb^{3+} is higher, the emission of $^5D_3 \rightarrow {}^7F_J$ transition gradually decreases to disappear, while the mainly factor was $^5D_4 \rightarrow {}^7F_J$ transition emission. This is due to the cross-relaxation between $^5D_3$ and $^5D_4$ [18], when the Tb^{3+} doping concentration is high, the average distance between Tb^{3+} and Tb^{3+} becomes shorter and shorter, and the energy will transfer from the $^5D_3$ level of one Tb^{3+} to the $^5D_4$ level of another Tb^{3+}. Thus, the $^5D_3 \rightarrow {}^7F_J$ transition emission is quenched, and the cross-relaxation process can be expressed as follows:

$Tb^{3+}(^5D_3) + Tb^{3+}(^7F_0) \rightarrow Tb^{3+}(^5D_4) + Tb^{3+}(^7F_0)$

From the excitation and emission spectra of Ce^{3+},Tb^{3+} double doped samples (b), it is shown that in the excitation spectra that under the monitoring of $^5D_4 \rightarrow {}^7F_5$ transition emission (542 nm) of Tb^{3+}, there are not only the excitation peaks of Ce^{3+} but also the excitation peaks of Tb^{3+}. This indicates that Tb^{3+} is essentially excited by Ce^{3+} , implying that $Ce^{3+} \rightarrow Tb^{3+}$ has an effective energy transfer, and that the excitation peak of Ce^{3+} at ~ 351nm is the strongest, which matches the emission spectrum of NUV-LED chip. The emission spectrogram excited at 351nm consists of two parts: the broadband emission of the 5d→4f transition of Ce^{3+} (400 ~ 480 nm) and the peak emission of the $^5D_4 \rightarrow {}^7F_J$ (J= 6, 5, 4, 3) of Tb^{3+}. From the characteristic transition emission intensity of Tb^{3+} in the two diagrams (a) and (b), it can be seen that the emission intensity of co-doped Tb^{3+} is 10 times that of single-doped Tb^{3+}. It is obvious that the significant enhancement of Tb^{3+} emission intensity is the result of $Ce^{3+} \rightarrow Tb^{3+}$ energy transfer.

Fig. 6 shows the emission spectra of $Ca_{0.95-x}Al_2Si_2O_8$: xCe^{3+}, $0.05Tb^{3+}$ ($0 \le x \le 0.06$) excited at 351nm. The fixed concentration of Tb^{3+} in all samples was 0. 05 mol, and the doping concentration of Ce^{3+} was changed. It can be seen from the diagram that with the increase of Ce^{3+} doping concentration, the emission intensity of Ce^{3+} gradually weakened while the emission intensity of Tb^{3+} increased gradually, which indicates that the introduction of Ce^{3+} has a process of energy transfer to Tb^{3+}. In this process, Tb^{3+} obtains partial excitation energy from Ce^{3+}, resulting in the enhancement of the $^5D_4 \rightarrow {}^7F_J$ (J= 6, 5, 4, 3) transition emission of Tb^{3+}. In addition, with the increase of Ce^{3+} concentration, the distance between Ce^{3+} and Tb^{3+} is getting closer and closer, and the energy transfer between the two ions increases gradually. Therefore, the emission intensity of Tb^{3+} is gradually enhanced. The small illustrations in Fig.6 shows the photo of the most luminous intensity sample $CaAl_2Si_2O_8$:$0.06Ce^{3+}$, $0.05Tb^{3+}$ irradiated by ultraviolet lamp. It can be seen that the sample emits very bright green light.

The above is a qualitative analysis of the possible energy transfer process in the system based on the experimental data. The mechanism of energy transfer will be studied below. The energy transfer between the sensitizer and the activator usually has three forms: radiation transfer (radiative reabsorption), electron cloud exchange, and the effect of the near field force of the multipole. The radiation transfer process is that if the energy of the radiation spectrum emitted by one ion coincides with that of another ion absorption spectrum, then the radiation light will be absorbed by another ion, and the energy transfer process will occur between the ions. That is, the transfer process of "radiation reabsorption". For the process of radiation reabsorption, the emission spectrum of sensitizer and the excitation spectrum of activator are overlapped or partially overlapped, but for rare earth ions, the f-f transition is linear, both emission and absorption intensity are relatively weak. Therefore, the energy transfer efficiency of the radiation reabsorption process is relatively low. In this system, there is a small overlap between the emission peaks of Ce^{3+} and the f-f transition absorption line of Tb^{3+}, so the radiation energy transfer between the sensitizer and the activator can be ignored. In the case of electronic cloud exchange, there is a very close distance between the activator and the sensitizer (< 4 Å), which means that there is a large overlap between the two electron cloud orbits. However, both Ce^{3+} and Tb^{3+} are reduced ions in this system. If the electron cloud exchange is to take place, a higher energy is needed [19]. It can be seen that it is impossible to achieve energy transfer by the action of the electron cloud exchange. Therefore,

the energy transfer mechanism of $Ce^{3+}\rightarrow Tb^{3+}$ in $CaAl_2Si_2O_8:Ce^{3+}$, Tb^{3+} system is mainly due to the action of the near field force of non-radiative multipole.

4. Conclusion

In the $CaAl_2Si_2O_8$ system, the luminescent properties of single doped Ce^{3+} and Tb^{3+} samples and the energy transfer mechanism of $Ce^{3+}\rightarrow Tb^{3+}$ in the double doped samples were studied. For the sample doped with Ce^{3+}, it has a strong absorption in the near ultraviolet region of 351nm. Its emission spectrum is a broad band with a main peak at 419 nm, which belongs to the 5d→4f of Ce^{3+}. It emits very strong blue light. The highest luminescence intensity of the sample is $CaAl_2Si_2O_8:0.06Ce^{3+}$. However, the absorption of Tb^{3+} doped samples in the near ultraviolet region is very weak and cannot be effectively excited by NUV-LED. Through Ce^{3+}, Tb^{3+} double doped samples, the green emission of Tb^{3+} is obviously enhanced, which is 10 times the luminescence intensity of the single doped Tb^{3+} sample, indicating that there is an effective energy transfer between Ce^{3+} and Tb^{3+}, and the mechanism of $Ce^{3+}\rightarrow Tb^{3+}$ energy transfer is studied, and the results show that there is an effective energy transfer between Ce^{3+} and Tb^{3+}. $Ce^{3+}\rightarrow Tb^{3+}$ energy transfer mechanism is mainly due to the non-radiative multipole near-field force.

Acknowledgments

This work was supported by the National Natural Science Foundations of China (Grant No.51462031), the Fundamental Research Funds for the Central Universities (Grant no. 31920170005), and the introduction of excellent talent Research Funds for the Northwest University for Nationalities (Grant No. xbmuyjrc201125).

References

[1] J M. M. Jiao, Y. C. Jia, W. Lü, W. Z. Lv, Q. Zhao, B. Q. Shao, H. P. You, $Sr_3GdNa(PO_4)_3F:Eu^{2+}$, Mn^{2+}: a potential color tunable phosphor for white LEDs, J. Mater. Chem. C. 2 (2014) 90 - 97.

[2] M. Krings, G.Montana, R. Dronskowski, C. Wickleder, α-$SrNCN:Eu^{2+}$-a novel efficient orange-emitting phosphor, Chem. Mater. 23 (2011) 1694 - 1699.

[3] V. Bachmann, C. Ronda, A. Meijerink, Temperature Quenching of Yellow Ce^{3+} Luminescence in YAG:Ce, Chem. Mater.21 (2009) 2077 - 2084.

[4] G.Y. Lee, J.Y. Han, W.B. Im, S.H. Cheong, D.Y. Jeon, Novel blue-emitting $Na_{(x)}Ca_{(1-x)}Al_{(2-x)}Si_{(2+x)}O_8:Eu^{2+}$ (x = 0.34) phosphor with high luminescent efficiency for UV-pumped light-emitting diodes, Inorg.Chem. 51 (2012) 10688 - 10694.

[5] S. P. Kuang, Y. Meng, J. Liu, Z. C. Wu, L. S. Zhao, A new self-activated yellow-emitting phosp -or $Zn_2V_2O_7$ for white LED, Optik. 124 (2013) 5517 - 5519.

[6] Y. H. Song, E. J. Chung, S. H. Song, M. K. Jung, K. Senthil, T. Masaki, D. H. Yoon, Enhancem -ent of photoluminescent properties of green-emitting $(Ba_{2-x}Sr_x)SiO_4$ silicate phosphor using $Eu_2O_3@B_2O_3$ core–shells for white LED applications, Mater. Lett. 110 (2013) 34 - 37.

[7] H. Y. Jiao, Y. H. Wang, $Ca_2Al_2SiO_7:Ce^{3+}$, Tb^{3+}: A White-Light Phosphor Suitable for White-Light-Emitting Diodes, J. Electrochem. Soc. 156 (2009) J117 - J120.

[8] G. Blasse, New luminescent materials, Chem. Mater. 1 (1989) 294 - 301.

[9] B. M. J. Smets, Phosphors based on rare-earths, a new era in fluorescent lighting, Mater. Chem. Phys. 16 (1987) 283 - 299.

[10] K. R. Laud, E. F. Gibbons, T. Y. Tien, H. L. Stadler, Cathodoluminescence of Ce^{3+}- and Eu^{2+}-Activated Alkaline Earth Feldspars, J. Electrochem. Soc. 118 (1971) 918 - 923.

[11] H. D. Grundy, J. Ito, The refinement of the crystal structure of a synthetic non -stoichiometric Sr feldspar, Am. Mineral. 59 (1974) 1319 - 1326.

[12] W. B. Im, Y. I. Kim, J. H. Kang, D. Y. Jeon, Luminescent and aging characteristics of blue emit -ting $(Ca_{1-x}, Mg_x)Al_2Si_2O_8:Eu^{2+}$ phosphor for PDPs application, Solid State Commun. 134 (2005) 717 - 720.

[13] Y. H. Wang, Z. Y. Wang, P. Y. Zhang, Z. L. Hong, X. P. Fan, G. D. Qian, Preparation of Eu^{2+}

and Dy^{3+} co-activated $CaAl_2Si_2O_8$-based phosphor and its optical properties, Mater. Lett. 58 (2004) 3308 - 3311.

[14] Y. H. Wang, Z. Y. Wang, X. P. Fan, G. D. Qian, P. Y. Zhang, F. A. Zhang, Synthesis of long afterglow phosphor $CaAl_2Si_2O_8:Eu^{2+},Dy^{3+}$ via sol-gel technique and its optical properties, J. Rare Earths. 23 (2005) 625 - 628.

[15] K. S. Sohn, Y. Y. Choi, H. D. Park, Y. G. Choi, Analysis of Tb^{3+} Luminescence by Direct Transfer and Migration in YPO_4, J. Electrochem. Soc. 147 (2000) 2375 - 2379.

[16] D. D. Jia, J. Zhu, B. Q. Wu, Luminescence and energy transfer in $CaAl_4O_7:Tb^{3+}$, Ce^{3+}, J Lumin. 93 (2001) 107 - 114.

[17] A. Nag, T. R. N. Kutty, Photoluminescence due to efficient energy transfer from Ce^{3+} to Tb^{3+} and Mn^{2+} in $Sr_3Al_{10}SiO_{20}$, Mater. Chem. Phys. 91 (2005) 524 - 531.

[18] G. Blasse, B. C. Grabmaier, Luminescent Materials, Springer-Verlag, Berlin, 1994.

[19] A. M. Srivastava, M. T. Sobieraj, A. Valossis, S. K. Ruan, E. Banks, Luminescence and Energy Transfer Phenomena in Ce^{3+}, Tb^{3+} doped $K_3La\ (PO_4)_2$, J. Electrochem. Soc. 137 (1990) 2959 - 2962.